Estuaries and Coasts (2022) 45:551–566
https://doi.org/10.1007/s12237-021-00988-1

Seasonal Variation of Methane Fluxes in a Mangrove Ecosystem in South India: An Eddy Covariance-Based Approach

Palingamoorthy Gnanamoorthy[1,2] · S. Chakraborty[3,4] · R. Nagarajan[1] · R. Ramasubramanian[1] · V. Selvam[1] · Pramit Kumar Deb Burman[3,4] · P. Partha Sarathy[5] · Mohd Zeeshan[2] · Qinghai Song[2] · Yiping Zhang[2]

Received: 20 August 2020 / Revised: 8 July 2021 / Accepted: 26 July 2021 / Published online: 15 August 2021

Abstract

The atmospheric methane (CH_4) concentration has increased in recent years due to natural and anthropogenic causes. Hence, it is essential to quantify the potential sources of CH_4 to understand the factors responsible for its fluxes on a local to regional scale through in situ observations. Coastal wetlands, particularly the mangrove ecosystems in the tropical and subtropical coasts, are significant sources of CH_4. In this study, we used an eddy covariance-based technique to measure the CH_4 fluxes in a mangrove ecosystem in Pichavaram, South India. The daily mean CH_4 flux ranged from 12 to 26 nmol m^{-2} s^{-1} during the wet season and from 6 to 20 nmol m^{-2} s^{-1} during the dry season. The monthly mean flux during the wet period was between 0.8 and 1.8 g CH_4 m^{-2} $month^{-1}$, and in the dry season, it was between 0.4 and 0.6 g CH_4 m^{-2} $month^{-1}$. The visual correlogram and structural equation modelling technique revealed that air temperature, creek water dissolved oxygen, soil organic carbon, and redox potential are important factors that control the CH_4 fluxes. The results suggest that the Pichavaram mangrove wetland acts as a source for CH_4. Our results also indicate that tidal inundation and seasonal variations in atmospheric temperature and water salinity are key factors affecting the CH_4 flux in the Pichavaram mangrove ecosystem.

Keywords Tropical mangroves · Eddy covariance · Methane efflux · Air temperature · Salinity · South India

Introduction

Methane (CH_4) is the second most abundant anthropogenic greenhouse gas (GHG) in the atmosphere (Myhre et al. 2013; Etminan et al. 2016; Allen et al. 2018), contributing to indirect warming with a radiative forcing of 0.48 Wm^{-2}. In contrast, carbon dioxide (CO_2) contributes about 1.66 Wm^{-2} (IPCC 2013; Myhre et al. 2013). Recent estimates have revealed that the CH_4 level in the atmosphere has increased 2.5 times from 720 ppb during the pre-industrial period (Etheridge et al. 1998). Methane is emitted from various sources, including wetlands, and during anthropogenic activities such as agriculture, power production, and urban waste disposal (Saunois et al. 2017; Turner et al. 2019; Rosentreter et al. 2021). The increase in atmospheric temperature (TAir) due to global warming leads to a rise in CH_4 emissions from these sources (Gedney et al. 2004; Ma et al. 2017; Zhang et al. 2017). Moreover, CH_4 concentrations have increased rapidly from 1775 to 1857 ppb between 2007 and 2018 (Nisbet et al. 2016, 2019; Saunois et al. 2020), and this trend is found to be strong in tropical and subtropical regions (Nisbet et al. 2016). In India, CH_4 observations and flux measurements are sparse; only a handful of such observations are available from a few urban and semi-urban areas (Ganesan et al. 2017; Guha et al. 2018; Tiwari et al. 2020). The available records show that the values are relatively high and display large seasonality, if compared with the observations in Mauna Loa in Hawaii and Seychelles in the Indian Ocean (Sreenivas

Communicated by Marco Bartoli

✉ Palingamoorthy Gnanamoorthy
pg.moorthy87@gmail.com; gnanamoorthy@xtbg.ac.cn

[1] Coastal Systems Research, M. S. Swaminathan Research Foundation, Chennai, India

[2] CAS Key Laboratory of Tropical Forest Ecology, Xishuangbanna Tropical Botanical Garden, Chinese Academy of Sciences, Menglun, China

[3] Centre for Climate Change Research, Ministry of Earth Sciences, Indian Institute of Tropical Meteorology, Pune, India

[4] Department of Atmospheric and Space Sciences, Savitribai Phule Pune University, Pune, India

[5] Centre of Advanced Study in Marine Biology, Annamalai University, Parangipettai, Tamil Nadu, India

et al. 2016; Metya et al. 2021a, b). Due to limited observational CH_4 flux data and the limited spatial scale of chamber-based measurements (Saunois et al. 2020), it is difficult to estimate a regional-scale CH_4 budget for India. Therefore, there is an urgent need to increase ecosystem-level data on CH_4 fluxes, adopting methods that integrate small-scale variability as the eddy covariance (EC) technique and focusing on ecosystems that store large amounts of organic carbon as wetlands.

Mangrove forests are important ecosystems in tropical and subtropical coasts and store large amounts of carbon in their sediments (Atwood et al. 2017). They are being used to mitigate the effects of climate change in many areas (Siikamäki et al. 2012; Wylie et al. 2016) as the rates of primary productivity are high in these forests (218 ± 72 TgC year^{-1}) (Bouillon et al. 2008) and they store vast amounts of carbon in their above- and below-ground biomass (Donato et al. 2011). However, the mangrove sediments produce GHGs, which are released to the atmosphere (Chen et al. 2014).

The anoxic conditions of sediments, their organic matter content (SOM), redox potential (Eh), and the hydrogeophysical environment are key potential drivers of CH_4 emission from mangrove forests. The anoxic conditions that prevail during the wet season cause more CH_4 production through methanogenesis than during the dry season (Jacotot et al. 2018). The decomposition of SOM depends on tidal inundation and rainfall that influence the Eh of the sediment, which in turn alters the rate of GHG emission (Kristensen et al. 2008a). Although mangrove forests act as a sink for CO_2 (Gnanamoorthy et al. 2020; Liu et al. 2020), the sediment and water in the creeks generally act as a source for CO_2 and CH_4, which are released to the atmosphere (Borges et al. 2003; Jacotot et al. 2018). Methane emission from mangrove soil is highly variable but generally higher than that from creek water. Moreover, enhanced emission has been observed in the locations where roots and pneumatophores are present (Sotomayor et al. 1994; Purvaja et al. 2004; Kristensen et al. 2008b).

A majority of the studies on mangrove CH_4 budget across the globe have focused only on sediment and aquatic fluxes (McNicol et al. 2017). In this regard, the soil-to-atmosphere CH_4 flux estimation showed broad variability, from 6 to 828 mmol m^{-2} day^{-1}, as observed by various investigators in India, Brazil, Puerto Rico, China, Taiwan, Tanzania, Thailand, and Australia using the static chamber technique (Lyimo et al. 2002; Chang and Yang 2003; Purvaja et al. 2004; Lekphet et al. 2005; Allen et al. 2007; Wang et al. 2016; Nobrega et al. 2016; He et al. 2019). The recent global estimates of CH_4 emission from mangrove sediments and from creek water are 0.315 ± 0.123 Tg CH_4 year^{-1} and 0.232 ± 0.059 Tg CH_4 year^{-1}, respectively (Rosentreter et al. 2018). All these studies only showed soil–water-atmosphere CH_4 fluxes attained from the static chamber, measured in spatially limited areas. Chamber-based methods, if not properly replicated, cannot provide precise estimates of CH_4 budgets due to large temporal and spatial variability of CH_4 fluxes (Wille et al. 2008; Jha et al. 2014). There is also a significant data gap in direct quantification of net CH_4 flux from an ecosystem, and the seasonal-scale variability is not well documented. Therefore, long-term, continuous, direct monitoring of ecosystem-scale CH_4 fluxes can improve our understanding and estimation of regional CH_4 budgets (Liu et al. 2020).

An EC flux tower provides an instantaneous trace gas exchange between the land surface and the atmosphere. This system is widely used in various ecosystems due to the advantage of direct and near continuous flux monitoring under natural, unmanipulated conditions (Baldocchi 2003; Aubinet et al. 2012). However, the CH_4 flux observation is still considered to be limited in comparison to CO_2 flux estimation (Knox et al. 2019). Recently, Liu et al. (2020) studied the CH_4 emission rate in the mangroves of the subtropical region of Hong Kong, China, using the EC technique. Such studies are rare in the Indian context, and to our knowledge, EC-based CH_4 flux estimation has been reported only from the mangrove ecosystem of the Sundarban delta using 2 months of EC data (Jha et al. 2014). To fill this gap, an EC flux tower was set up in the south Indian mangrove wetland of Pichavaram under the MetFlux India Project (Deb Burman et al. 2020; Chakraborty et al. 2020). The main objective of this study is to examine the diurnal and seasonal (dry and wet periods) variations in CH_4 fluxes using the EC method and their relationship with various environmental and physico-chemical parameters that control CH_4 emission in a mangrove environment.

Materials and Methods

Research Site

The research work was conducted in the mangrove forest located in the Cauvery Vellar-Coleroon estuarine (wetland) region of Pichavaram (Vellar and Coleroon) (lat. 11° 25′ 36″ N; long. 79° 47′ 38″ E) (Fig. 1). The mangrove ecosystem cover pattern shows that 813 ha are covered by the naturally dense mangrove forest, 68 ha by sparse mangrove, 664 ha by marshy vegetation, and 340 ha by mudflats. The mangrove wetland is comprised of 51 small islands colonised by mangrove plants (Selvam et al. 2002). Nearly 12 true mangroves species exist in the study area. There are two distinct distribution zones of mangrove species: the *Rhizophora* spp. zone and the *Avicennia* spp. zone. The *Rhizophora* spp. zone is found in the fringes of the creeks and is narrow in width (6–18 m). The *Avicennia* spp. zone makes up the interior of the forests and ranges in width from 60 to 80 m. The height

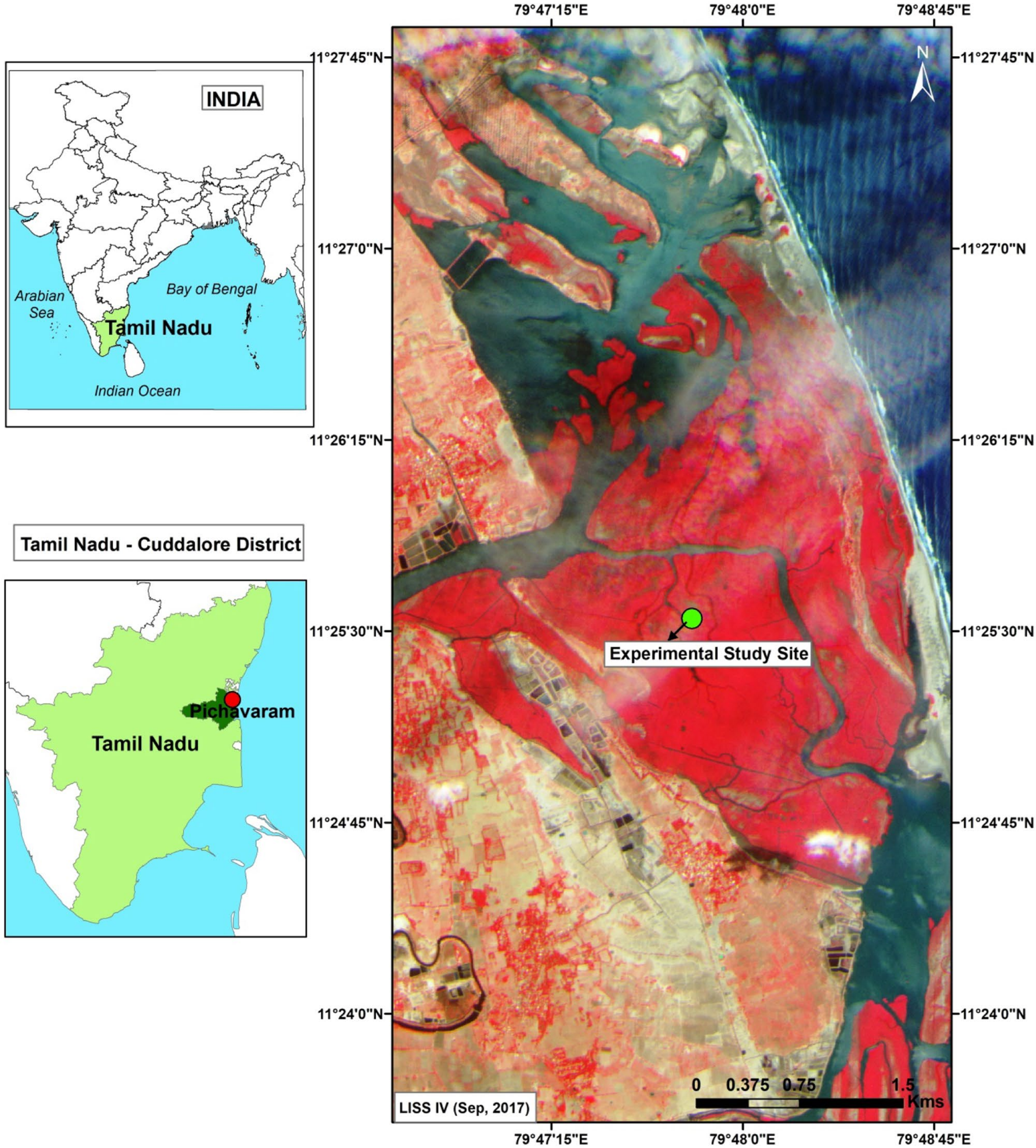

Fig. 1 The study area map indicates the EC flux tower location using a light green circle on the right-side panel. The upper-left portion shows the map of India, while the green-shaded area in lower left denotes the state of Tamil Nadu. A zoomed-in version of the research site is shown on the right side, where the red colour indicates the Pichavaram mangroves

of the mangrove trees varies between 3 and 7.5 m. The mean leaf area index (LAI) in *Rhizophora* spp. is 4 m^2 m^{-2}, and for the *Avicennia* zone, it is 2 m^2 m^{-2}. The water column in the creeks is generally shallow, ranging between 0.3 and 3.0 m (Selvam 2003). The Pichavaram mangrove wetland is hot in the summer months and relatively cooler during the post-monsoon period (Kathiresan 2000). It experiences dry conditions during April–August and wet conditions during September–November (the monsoon season). The peak rainfall occurs during the northeast monsoon season

(October–December) in the southeastern part of peninsular India (IMD 1973; Rajeevan et al. 2012), which is characteristically different from other parts of India. The tidal table predicted for the nearest location of the EC tower is the Cuddalore Port, India. The period of inundation for Pichavaram has been derived using the tides4fishing software package.

Eddy Covariance Tower and Instrumentation

The iron-based, triangle-shaped (10 m height) flux tower was erected in the observation site to monitor the CH_4, CO_2, and H_2O and energy fluxes in 2016. The EC flux tower is encircled by abundant natural mangrove vegetation with prevailing species such as *Rhizophora mucronata*, *R. apiculata*, and *Avicennia marina*. The canopy height ranges from 3 to 4 m. Three solar-power systems ensure uninterrupted power supply to the sensors (one 24 V and two 12 V power output) using batteries (500 AH). The CH_4 flux measurements were carried out at the 10-m level. A three-axis ultrasonic anemometer (Wind Master Pro, Gill Instruments Limited, Hampshire, UK) measured the high-frequency wind velocity and sonic temperature (T_s), and the open path methane analyser (model: LI-7700, LI-COR Biosciences, NE, USA) measured atmospheric CH_4 concentration. The raw data from the anemometer and open path methane analyser were logged by an analyser interface unit (model: LI-7550, LI-COR Biosciences, NE, USA) at the rate of 10 Hz. The supplementary environmental parameters were also monitored above the canopy at 10-s interval, averaged over 30 min, and logged on a CR3000 data logger (Campbell Scientific Inc., Logan, UT, USA). The meteorological parameters – net radiation (using a net radiometer; model: NR01, Hukseflux, Netherlands) and photosynthetic active radiation (PAR) (model: SQ-100 and 300 series, Apogee instruments Inc., UT, USA) – were measured at the 6-m level. Further meteorological parameters, such as air temperature, relative humidity, wind direction, wind speed, and rainfall, were measured at various levels, namely, 2 m, 6 m, and 10 m (using a Vaisala weather transmitter; model: WXT520, Helsinki, Finland). The soil heat flux was monitored at two depths (2.5 cm and 5 cm) (model: HFP01SC-20, Hukseflux, Netherlands). The LAI was recorded using a portable LAI-2200 plant canopy analyser in the four different directions of each location (LI-COR Biosciences, NE, USA). An enclosed path infrared gas analyser (IRGA) sensor (model: Li-7200, LI-COR Biosciences, NE, USA) was also used to measure the CO_2 concentration and its fluxes. The results of CO_2 fluxes are presented in Gnanamoorthy et al. (2020).

CH_4 Flux Data Analysis

The EC technique is considered to be a reliable method of estimating CH_4 fluxes in the mangrove (Liu et al. 2020) and other ecosystems (Knox et al. 2019).

The following successive equation is used to compute CH_4 fluxes (Baldocchi 2003):

$$fCH_4 = \overline{\rho_\alpha} \bullet \overline{\omega' s'} \quad (1)$$

where fCH_4 is the CH_4 flux (nmol m^{-2} s^{-1}); ρ_α is the air density; ω' and s' are vertical wind speed and the CH_4 concentration variations, respectively; and the over bar in the equation denotes the averaging time of 30 min.

The collected raw EC data (from April 2018 to November 2018) were processed using the EddyPro software (6.1.0, LI-COR Biosciences, NE, USA); this gave the values for concentration and fluxes of CH_4 averaged on a 30-min time frame. The raw flux data usually contain different kinds of noises, and hence, they are subjected to a variety of correction schemes to obtain reliable data. The FLUXNET community has developed protocols that employ various correction schemes (Baldocchi et al. 2001; Reichstein et al. 2005), which we have followed here and are described in Table 1.

Further processing is done to eliminate sensor errors and unusual atmospheric situations, such as heavy rain events (Liu et al. 2020). The night-time fluxes are underestimated due to low turbulence (Baldocchi 2003). To address this issue, the friction velocity (u*) threshold is fixed at 0.13 ms^{-1}, and data beyond this limit are excluded using an average value test technique (Zhu et al. 2006). The received signal strength indicator (RSSI) is a measure of the cleanliness of the mirrors of the CH_4 sensor. Data having RSSI

Table 1 Methods used to calculate the 30-min flux measurements in the EddyPro software

Flux data correction scheme	References
Triple-coordinate rotation to eliminate errors due to sensor tilt and non-homogenous terrain at the site	Baldocchi et al. (2000); Wilczak et al. (2001)
WPL calibration to compensate air-density variations	Webb et al. (1980)
Removal of large spikes due to instrument error and unrealistic values	Sabbatini et al. (2018)
Quality control tests for the flux values	Foken et al. (2004); Göckede et al. (2008)
Flux footprint estimation	Kljun et al. (2004); Kormann and Meixner (2001)

lower than 20% are considered imprecise and hence rejected (Fortuniak et al. 2017).

Gap Filling of CH_4 Fluxes

Estimation of continuous time series of the flux data using EC is difficult due to several reasons, such as low turbulence, extreme rain events, and technical snags, for example, power and sensor malfunction. No standard universal method is currently available to fill the gap for the CH_4 fluxes (Nemitz et al. 2018). To generate continuous time series on the daily and monthly scale of CH_4 fluxes, we used the marginal distribution sampling (MDS) method for gap filling algorithm (Reichstein et al. 2005; Papale et al. 2006), which is considered a reliable method by the FLUXNET community and is incorporated in the REddyProc package (Wutzler et al. 2018).

As this method is used widely for gap filling of CO_2 and H_2O fluxes (Deb Burman et al. 2021), the MDS algorithm can be used for CH_4 fluxes as well (Rinne et al. 2007; Meijide et al. 2011; Hatala et al. 2012a, b; Alberto et al. 2014; Ge et al. 2018; Tang et al. 2018).

Estuarine Soil and Water Parameters

In addition to the EC data, soil samples were collected bimonthly from three locations in and around the flux tower footprint area, encompassing the natural mangrove stands. Mangrove soil was collected at the following depths using a stainless steel corer: 0–15 cm, 15–30 cm, 30–60 cm, and 60–90 cm. The sampled soil was stored in plastic bags and then transported to the laboratory for further analysis. Soil parameters such as temperature (TSoil), pH, Eh, and salinity (soil sal) were measured in the field using digital pH, Eh, and electrical conductivity metres (Hanna instruments). The soil organic carbon (SOC) was estimated using the Walkley–Black (WB) method (Walkley and Black 1934).

Surface water samples from the creek canal at four different locations around the flux tower were collected once a week using a Niskin water sampler and transferred in clean borosilicate bottles. We used a water quality monitoring system (Hydrolab Quanta Multi-Probe Meter, TX, USA) to measure in situ water temperature (WT), dissolved oxygen (DO), and salinity (Wsal). The pH was measured at three-digit precision using a pH metre (EUTECH waterproof, cyber scan pH-610-pH/mV/temperature metre-ECPH-WP61042K) calibrated on the NBS scale. The biological oxygen demand (BOD) was measured using Winkler's method. Chlorophyll "a" (Chl) was analysed using the method outlined by Strickland and Parsons (1972). The total alkalinity (Talk) was determined by the standard method of Gran titration (Gran 1952). We filtered the water sample through a cellulose acetate filter paper (0.45 μm) to measure the alkalinity. The filtered water was stored in 250-mL borosilicate bottles, and 100 μL of saturated mercuric chloride solution was added to arrest microbial growth (Cai and Wang 1998; Jiang et al. 2008). While collecting the creek water, all sampling bottles were allowed to overflow for at least twice their volume to reduce contact with the air. Afterwards, the sampled bottles were stored at 4 °C for further analysis. For total dissolved inorganic carbon (DIC) and dissolved organic carbon (DOC) measurements, water samples were collected using separate clean high-density (HD) polythene bottles and stored in an icebox. Total organic carbon (TOC) and DOC were measured using an automated TOC analyser (Innoax Lab 0463). Particulate organic carbon (POC) was obtained using GF/F84 filters (0.45 μm), dried at 65 °C, and analysed on elemental analyser (Perkin Elmer 2400).

Statistical Analysis

The statistical analyses (linear regression) were carried out using the Origin software (version 2018, Origin Lab Co., Northampton, MA, USA). Visualisation of a correlation matrix graph was generated using a package "Performance Analytics" of the R Team Cooperation (Peterson et al. 2018). Finally, the fitting of the structural equation model (SEM) was accomplished using the Amos 21.0 software (IBM, Armonk, NY, USA). The SEM is a multivariate statistical analysis technique which, in this case, describes how the CH_4 fluxes were influenced by the environmental parameters in the mangrove ecosystem. The goodness of model fit (Hou et al. 2004) was determined to test the robustness of the result. The index includes CMIN/DF (minimum discrepancy divided by degrees of freedom), root mean square error of approximation (RMSEA), Bentler–Bonett normed fit index (NFI), comparative fit index (CFI), goodness-of-fit index (GFI), incremental fit index (IFI), Akaike information criterion (AIC), and expected cross-validation index (ECVI).

Results

Atmospheric and Estuarine Parameters

Meteorological parameters varied monthly over the study period (Fig. 2a–c). The mean monthly TAir during the study period varied from 27.3 (November 2018) to 31 °C (June 2018), while the monthly TSoil ranged from 26.8 (November) to 30.5 °C (June) (Table S1). The relative humidity varied from 30 to 99%. The daily maximum net radiation on the measurement days varied between 412.4 and 906 Wm^{-2}. The total precipitation was 351 mm, with the highest rainfall (113 mm) observed in November (Fig. 2c). The noon time mean PAR was highest in the hot season (April–July; range: 1482–1911 $\mu mol\ m^{-2}\ s^{-1}$) and lower in the wet season

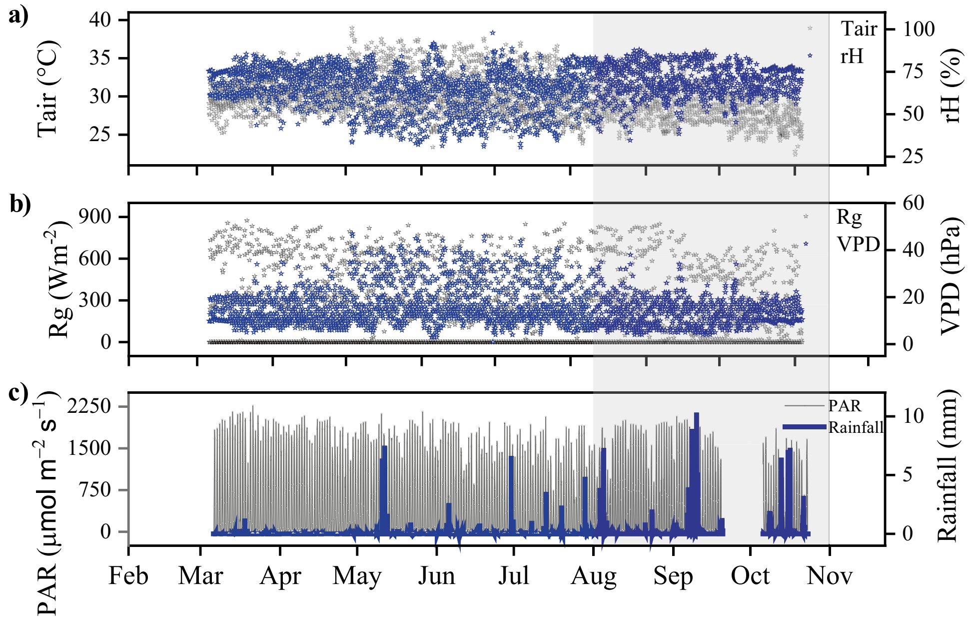

Fig. 2 Half-hour time series of (**a**) atmospheric temperature (TAir) and relative humidity (rH); (**b**) net radiation (Rg) and vapour pressure deficit (VPD); (**c**) photosynthetic active radiation (PAR) and averaged daily rainfall data from April 2018 to November 2018. The grey shade indicates the wet season and the white area of each panel indicates the dry season

(October–November; range: 1397–1603 µmol m^{-2} s^{-1}). Other measured environmental parameters were temperature, pH, salinity, Talk, DO, BOD, Chl, TOC, DIC, DOC, and POC for water and temperature, pH, salinity, Eh, and SOC for soil (Table S1).

Diurnal and Seasonal Variability of the CH_4 Fluxes

Figure 3a shows the seasonal variation of CH_4 fluxes. Higher values were observed in the wet season. The mean daily fluxes, regardless of the months and time of day, are mostly positive, indicating the ecosystem is a net CH_4 source (Fig. 3a, c). A typical diurnal pattern of CH_4 flux was observed: maximum post-noon (13:00–16:00 h) and minimum in the early morning (1:00–6:00 h) and evening (19:00–21:00 h) (Fig. 3c). During the dry season (April–August) and wet season (September–November), the daily maximum CH_4 flux was observed in the post-noon. The average daily variability of CH_4 flux was lower in the dry season (6.4 ± 4.1 nmol m^{-2} s^{-1}) and higher during the

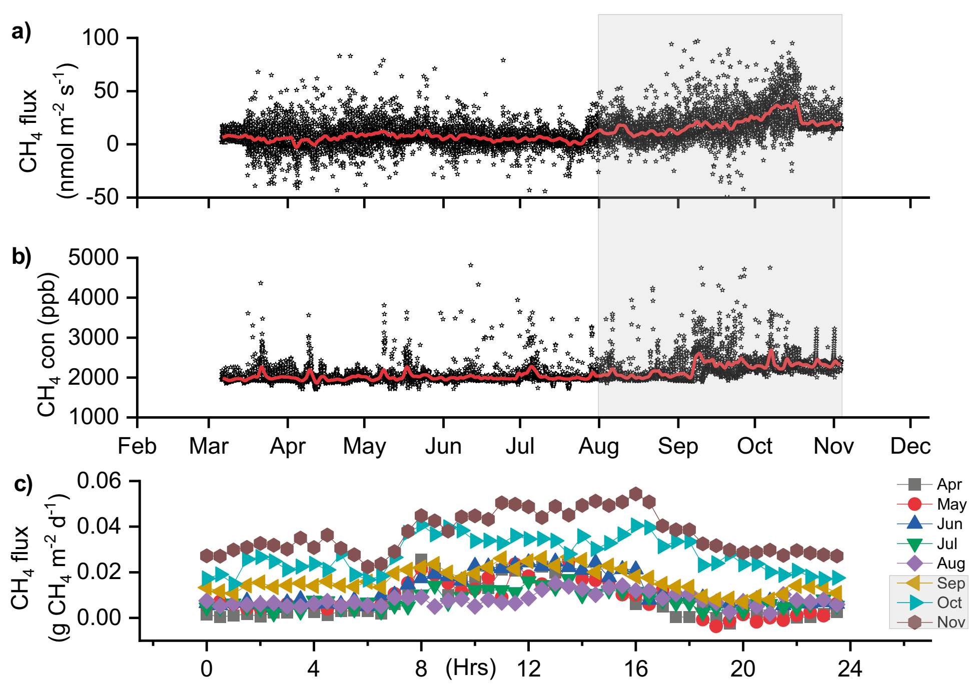

Fig. 3 Half-hour continuous (**a**) methane (CH_4) flux and (**b**) CH_4 concentration (CH_4 con) are plotted on a monthly scale and (**c**) mean monthly diurnal (24 h) patterns of CH_4 flux. Mean diurnal flux was calculated based on the sum of the average hourly CH_4 flux multiplied by the total days in the month (**c**). Red-colour streaks in panels (**a**)–(**b**) indicate daily means. The grey shade indicates the wet season, and the white area of each panel indicates the dry season (**a**–**b**)

wet season (19.63 ± 5.3 nmol m^{-2} s^{-1}) (Fig. 3c). The highest values recorded in October and November were 1.33 and 1.77 g CH_4 m^{-2} $month^{-1}$, respectively. The values observed during April–August were low, between 0.36 and 0.59 g CH_4 m^{-2} $month^{-1}$.

The mean daily CH_4 concentration in the study area was 2098 ± 275 ppb (Fig. 3b). The maximum mean daily value of 2346 ppb was recorded in November and the minimum of 1980 ppb during May. The diurnal patterns of CH_4 concentration reached a maximum value in the morning hours (04:00–07:30 h) and minimum post-noon (13:00–16:00 h), and it was opposite to CH_4 flux values. The averaged CH_4 concentration during the dry and wet periods was 2009 ± 183 ppb and 2248 ± 336 ppb, respectively.

Footprint Analysis

We calculated the footprint of the CH_4 fluxes to characterise the flux source area in the mangrove forest, as suggested in Baldocchi (1997). The footprint calculation was demonstrated using a parameterisation scheme outlined by Kljun et al. (2004). The wind rose diagrams (Fig. 4a–c) illustrate the predominant wind direction and footprint, and the CH_4 concentration is calculated to get the location of the EC flux measurements. The estimated footprint or fetch (90%) varied from 118 to 448 m, with a mean distance of 204 m from the EC tower (Fig. 4a). The dominant wind direction at the research site was southwest-west-northwest (Fig. 4b), and the wind speed was between 1.05 and 7.1 m s^{-1} with a mean value of 2.5 m s^{-1} during the entire study period (Fig. 4c).

The CH_4 flux was recorded predominantly from the west, and especially from the southwest, with values of 11–30 nmol m^{-2} s^{-1} (Fig. 4c). Significantly higher values of CH_4 fluxes (40 nmol m^{-2} s^{-1}) have been observed with westerly/southwesterly airflow due to the presence of dense mangrove vegetation (Fig. 4c). The distribution of mean CH_4 concentration depends on the wind direction, which has been calculated for the whole study period (Fig. 4b). Higher CH_4 concentration from the natural mangrove forest was observed when the wind speed was low (< 2 ms^{-1}) (Fig. 5). The relationship between CH_4 concentration and wind direction was the same as CH_4 flux values throughout the study period, while the monthly averaged CH_4 concentration values were between 1980 and 2346 ppb (Fig. 4c).

Estuarine Factors Controlling the CH_4 Fluxes

Figure 5a–b show the CH_4 fluxes with respect to tidal inundation as it is one of the most important factors controlling the fluxes (Purvaja and Ramesh 2001). Methane flux varies highly depending on tidal inundation patterns. The study site receives two high tides and low tides every day (semi-diurnal tides). The CH_4 flux was relatively higher during the low tide than during the high tide condition. During low tide, CH_4 emissions reached a maximum at the beginning of the rising tide and continued until the end of the tide (Fig. 5). The results suggest that high CH_4 flux was observed after high tide patterns during both dry and wet seasons. Figure 6a shows a reasonably good negative correlation between CH_4 flux and water salinity ($R^2 = 0.27$, $p < 0.05$). This tendency was only partly sustained when the data were grouped by salinity class. The averaged CH_4 emission was significantly lower for euryhaline conditions (> 40) than for mesohaline conditions (5–18). Oligohaline conditions (0.5–5) showed considerably higher efflux than both euryhaline and mesohaline conditions. The peak variability overlapped with the highest emission in the salinities between 3 and 5. The relationship between CH_4 flux and air temperature showed increasing CH_4 fluxes with increasing temperature ($R^2 = 0.60$, $p < 0.05$; Fig. 6b).

Both CH_4 flux and CH_4 concentration showed negative correlations with air temperature, soil temperature, WT, wind direction, soil pH, and POC as illustrated in the correlogram (Fig. 7). While CH_4 flux was positively correlated with Eh and chlorophyll, CH_4 concentration showed a positive correlation with CH_4 flux and chlorophyll content in the water (Fig. 7).

Structural Equation Modelling

Based on the features of CH_4 flux from the mangrove forest, a conceptual model of the major factors affecting CH_4 fluxes and CH_4 concentration has been established (Fig. 8). The SEM contains two latent variables (CH_4 flux and CH_4 concentration) and five quantifiable variables (DO, Eh, TAir, Wsal, and SOC). Typical model fitting index analysis was predicted using conceptual models and assumptions; the primary model was tailored using Amos 21.0 (IBM SPSS). By successive frequent fitting, evaluation, and alteration of the model, the concluding normalised coefficient correction model with better fitting indices was attained (Fig. 8; Table 2). The SEM, absolute fitting index, relative fitting index, and reduced index were used in this study on the basis of earlier endorsements (Fang et al. 2019; Hou et al. 2004). The output of the fitting index investigation for the model is given in Table 2. The fitting index of the model was usually acceptable, meeting all fitting index necessities. The relationship model of CH_4 efflux in mangrove forests attained using the statistical technique was reasonable. Methane flux was significantly affected by Eh and CH_4 concentration ($p < 0.05$) but not by SOC and TAir ($p > 0.05$), and the respective path coefficients were 1.92 and 0.96 indicating the significant impact of mangrove forests on flux

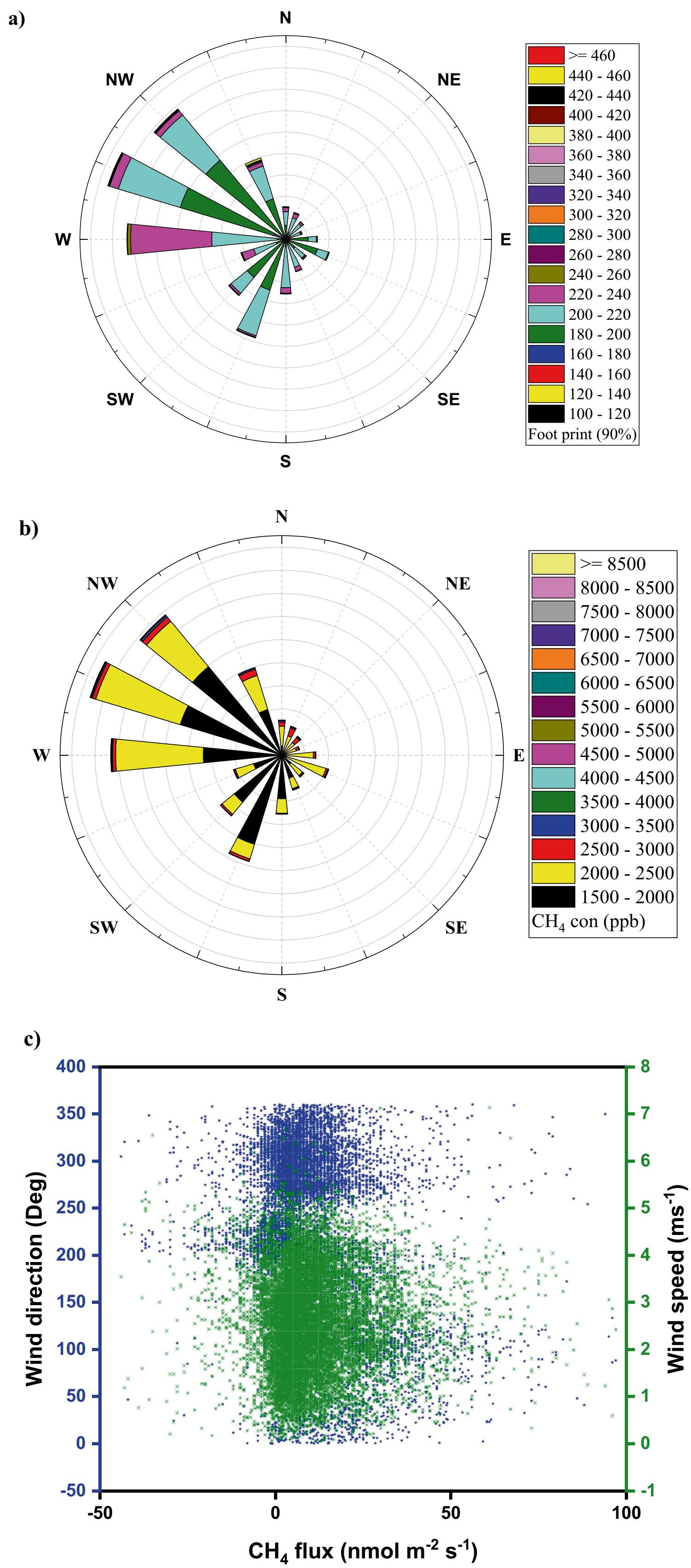

Fig. 4 (**a**) Wind rose and fetch of the eddy covariance (EC) system. The wind rose figure displays the footprint (fetch) and direction at the research site. Specifically, the stripes reveal the direction, while the colours indicate the maximum footprint value of 90%. (**b**) Methane concentration (CH_4 con) and direction calculated for the research site. The stripes display the direction, while the colours show the CH_4 concentration variations. (**c**) CH_4 flux in relation to wind speed and wind direction during the research period. Green and blue colours indicate the wind speed and direction, respectively

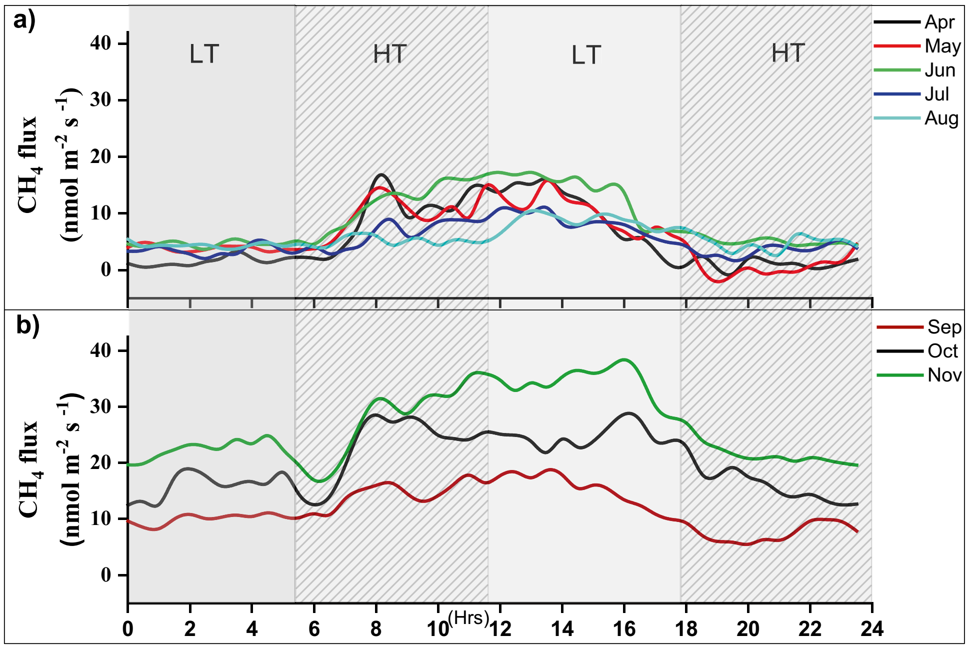

Fig. 5 The effects of high tide (HT) and low tide (LT) on diurnal methane flux during the dry season (**a**) and the wet season (**b**) in the Pichavaram study site. The x-axis represents the daily hours (h)

exchange rate (Fig. 8). Furthermore, water salinity was the most significant factor controlling CH_4 concentration (path coefficient −0.68; $p < 0.01$), whereas SOC and TAir were non-significant ($p > 0.05$). More significant relationships were found between the parameters for Eh and DO and for water salinity and DO (path coefficients 0.82 and −0.65, respectively; $p < 0.001$).

Discussion

Biogeochemical processes in mangrove ecosystem are complex and small-scale spatial and temporal variability, which makes the estimation of ecosystem-level CH_4 fluxes complicate (Barr et al. 2010; Jha et al. 2014; Liu et al. 2020). In the past, the chamber-based method was

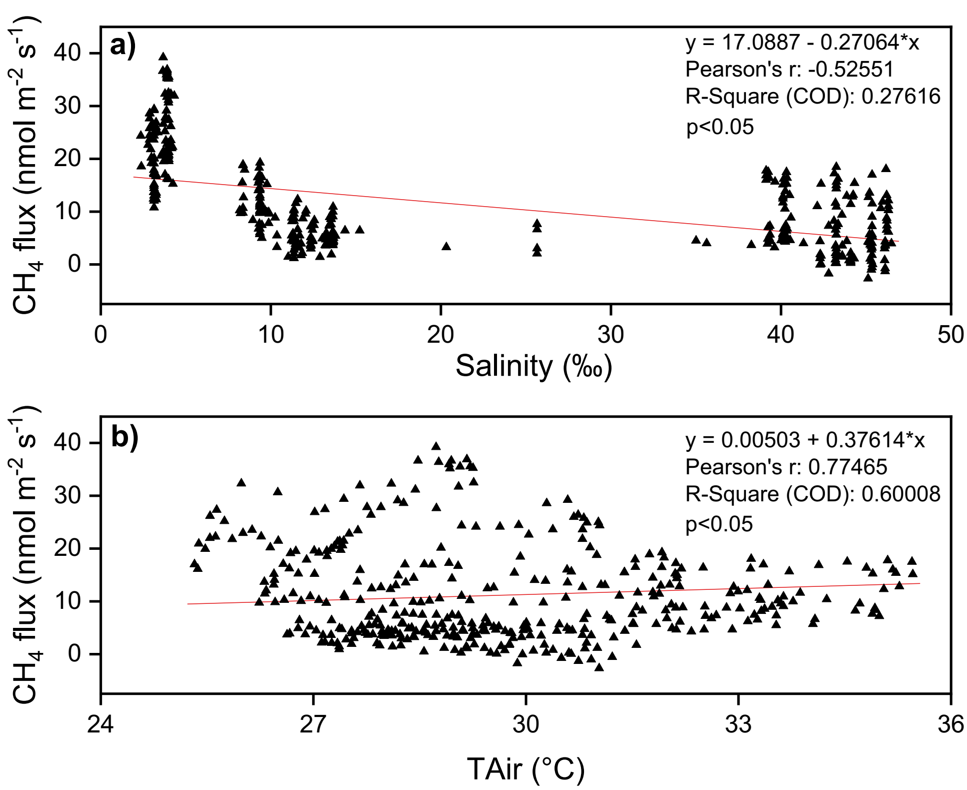

Fig. 6 Correlation between the salinity (**a**) and air temperature (**b**) with the methane flux observed in the study site

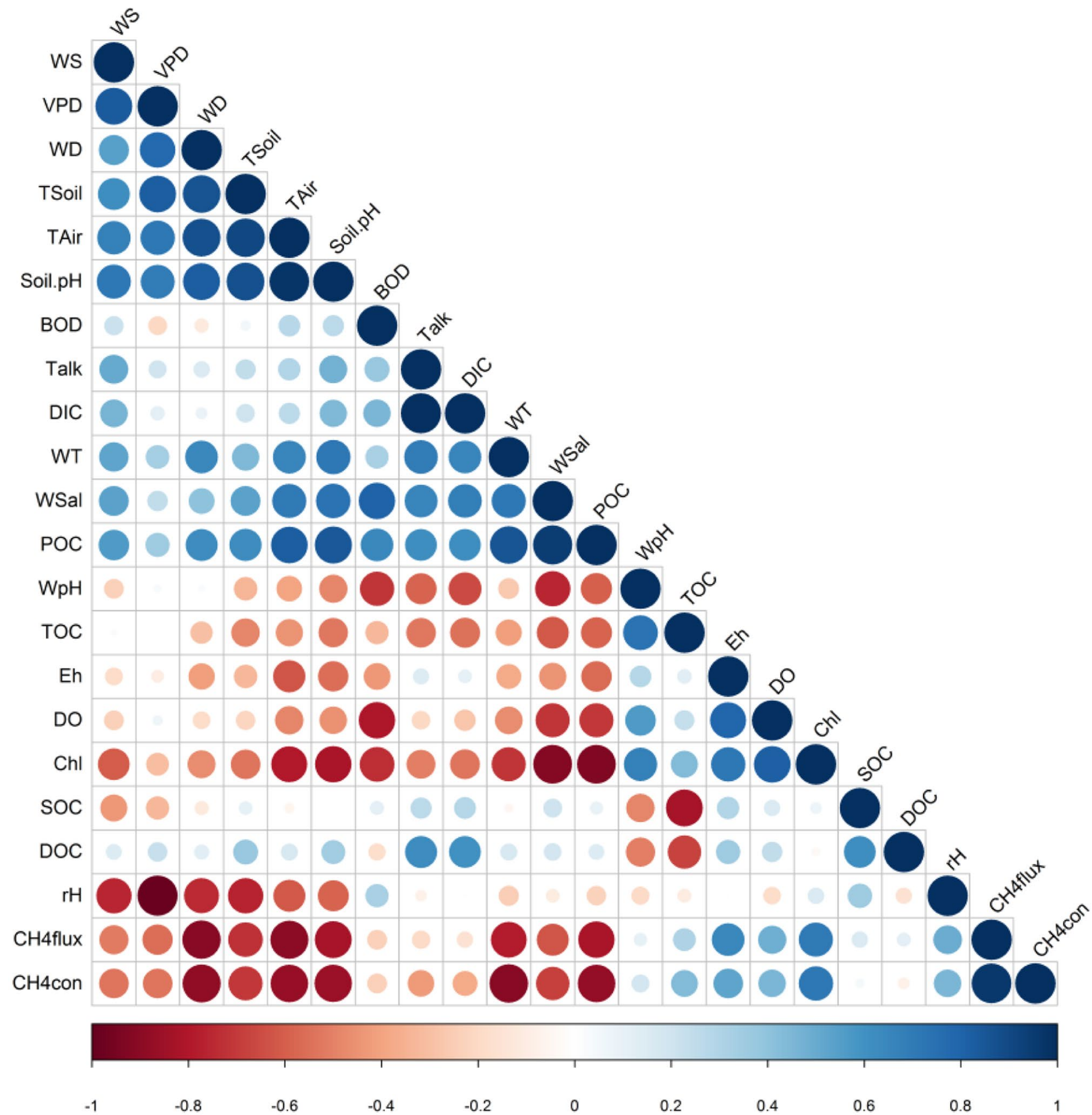

Fig. 7 Correlation matrix of the methane (CH_4) emissions against atmospheric/soil/water index. Positive correlations are displayed in blue and negative correlations in red. The colour intensity and the size of the circle are proportional to the correlation coefficients

widely used to estimate the CH_4 fluxes between soil and atmosphere to measure the fluxes on a plot-base (field) scale or field survey in several ecosystems (Livingston and Hutchinson 1995; Purvaja and Ramesh 2001; Acosta et al. 2019). The EC method is an advanced technique that provides a more precise estimation of fluxes from a large area, especially from natural forest ecosystems and agricultural wetlands (Baldocchi 2014; Petrescu et al. 2015; Morin 2018; Knox et al. 2019).

The published CH_4 emissions, using EC and the closed static chamber technique, from subtropical and tropical mangroves are highly variable (Table 3). The highest daily CH_4 flux measured via EC was observed during the summer months in the Sundarban mangroves in east India (Jha et al. 2014). Methane fluxes from the Sundarbans are likely higher than those measured in the Pichavaram mangroves because seasonal rainfall pattern, tidal inundation range, and temperature in the latter are different from those in the Sundarbans.

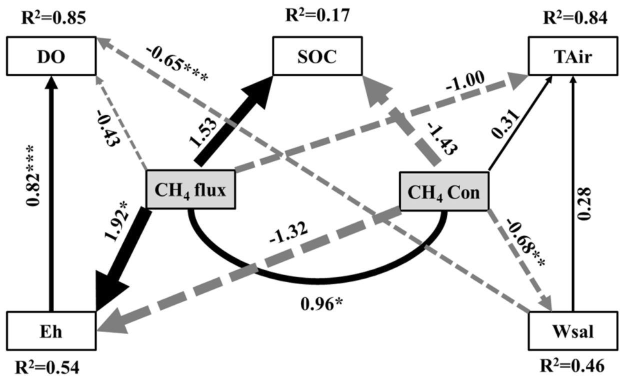

Fig. 8 Standardised coefficients correction model for key driving features of methane (CH_4) efflux from mangrove forests: the structural equation model (SEM) considered plausible pathways through which dissolved oxygen (DO), soil redox potential (Eh), air temperature (TAir), water salinity (Wsal), and soil organic carbon (SOC) influence CH_4 flux and concentration. The arrow width indicates the strength of standardised path coefficients. The solid black line arrows and the grey dashed lines represent positive path coefficients and negative path coefficients, respectively. Numbers on the arrow indicate significant standardised path coefficients (*$p<0.05$; **$p<0.01$; ***$p<0.001$) proportional to the arrow width. R^2 indicates the variance of endogenous variable explained by the model. $\chi2=4.908$, df = 9, probability level = 0.842, RMSEA = 0.000

Moreover, in the same study site, the closed static chamber studies also reported a higher rate of CH_4 emission than that reported by the present study (Purvaja and Ramesh 2001; Purvaja et al. 2004). Most of the chamber-based data showed higher rates of CH_4 emission in the mangrove wetland due the measurement techniques which allows for a buildup of CH_4 inside the chamber volume, when compared with emissions measured by the EC method (Allen et al. 2007; Konnerup et al. 2014; He et al. 2019). In contrast, lower CH_4 flux ranges were also observed by micrometerological and chamber methods in the Indian Sundarban mangroves (Mukhopadhyay et al. 2002; Biswas et al. 2007). Most of the previous estimations of CH_4 emission rates were done using closed static chamber techniques, which are relatively less precise due to smaller area and discontinuous estimations in terms of temporal and spatial variability (Pavelka et al. 2007; Jha et al. 2014). Reported CH_4 effluxes in a subtropical mangrove forest in Hong Kong, China, were higher in the dry as compared to the wet season, which contrasts our findings, but the mean CH_4 flux rate was comparable with our results (Liu et al. 2020). All these findings show that mangrove forests are not a strong source of CH_4 due to the inhibiting influences of sulphate and salinity (Purvaja and Ramesh 2001; Livesley and Andrusiak 2012).

CH_4 emission rates are high, particularly during the wet season (Purvaja et al. 2004; Zheng et al. 2018). Correspondingly, the overall average monthly CH_4 fluxes, presented as part of the present study, generally increased from August onwards, and the maximum change was observed in November, coinciding with the northeast monsoon (Fig. 3a, c). The studies conducted on these factors suggest that the CH_4 fluxes depend on seasons and abiotic factors such as soil type, soil temperature, water salinity, soil pH, Eh, tidal patterns, and soil moisture. Similarly, biotic factors such as vegetation, microbial diversity, and micro- and macro-algal mats on the sediment also control the CH_4 fluxes (Biswas et al. 2007; Allen et al. 2007; Purvaja et al. 2004; Krithika et al. 2008; Dutta et al. 2013; Bai et al. 2014; Jha et al. 2014; Chauhan et al. 2015; Wang et al. 2016). Methanogenesis is associated with anoxic environments which are most likely to occur during the wet season (Großkopf et al. 1998; Schwarz et al. 2007). During the monsoon season, anthropogenic organic matter from agriculture runoff and aquaculture farm organic waste discharging into the mangroves are additional sources of substrate for the methanogenic bacteria, which are liable for CH_4 emissions (Krupadam et al. 2007). Hence, to reduce CH_4 emissions, the anthropogenic input, particularly aquaculture waste discharged into the mangrove wetland from adjoining shrimp farms, should be diminished (Purvaja and Ramesh 2001). In the present study, CH_4 emissions were at their peak during the wet season and then dropped during the dry season. The months of August and September, representing a transition period from the dry to the wet season, showed a sharp increase in soil respiration, resulting in increased CH_4 fluxes (Gnanamoorthy et al. 2019). Intense emissions occurred in the wet season resulting in a higher variability due to the inundation of mangrove soil during the monsoon and spring tides. The influence of tides and freshwater significantly contributes to the CH_4 emission in the mangroves, but limited studies are available in this regard (Barnes et al. 2006; Purvaja et al. 2004; Kristensen et al. 2008b; Chauhan

Table 2 Structural equation model coefficients fitting indices

Model fitting index		Evaluation standard	Output results
Absolute fitting indices	CMIN/DF	< 3	0.545
Relative fit indices	NFI	> 0.9	0.920
	CFI	> 0.9	1.000
Compact indices	IFI	> 0.9	1.079
	AIC	The smaller, the better	56.908
	ECVI	The smaller, the better	8.130

Table 3 Reported methane fluxes in the mangrove wetlands of the tropical and subtropical regions (daily and hourly fluxes are presented for static chamber and eddy covariance measurements, respectively)

Measurement techniques	Mangrove sites	Range/mean values (g CH_4 m^{-2} day^{-1})	Reference
Static chamber	Pichavaram, India	47.23–324.48	Purvaja and Ramesh (2001)
Micrometeorological	Sundarban, India	–16–32	Mukhopadhyay et al. (2002)
Static chamber	Pichavaram, India	7.4–63.7	Purvaja et al. (2004)
Static chamber	Sundarban, India	0.032–2.15	Biswas et al. (2007)
Static chamber	Pichavaram, India	15.04–23.83	Senthilkumar (2008)
Eddy covariance	Sundarban, India	150.22	Jha et al. (2014)
Eddy covariance	Mai Po Nature Reserve mangrove, Hong Kong SAR, China	40	Liu et al. (2020)
Eddy covariance	Pichavaram, India	8–37	Present study
	Mangrove sites	Short-term values (mg CH_4 m^{-2} h^{-1})	Reference
Static chamber	Chelmer, Southeast Queensland, Australia	0.003–17.37	Allen et al. (2007)
Static chamber	Ciénaga Grande de Santa Marta, Colombia	0–31.57	Konnerup et al. (2014)
Static chamber	Dongzhaigang National Nature Reserve, China	0.84–5.49	He et al. (2019)
Eddy covariance	Pichavaram, India	0.326–1.538	Present study

et al. 2015). Our study reported 6–14% higher in concentration of CH_4 emission than the values observed by Metya et al. (2021a) from Sinhagad a hilly area in western India. Further, it varies with a study from Sundarban mangroves wherein emission was lower by 25% (Jha et al. 2014).

In mangrove wetlands, abiotic and biotic factors are recognised as controlling aspects of CH_4 emissions (Jha et al. 2014; Liu et al. 2020). Though both abiotic and biotic factors influence CH_4 emissions, seasonal factors are the main influencers of CH_4 efflux. If CH_4 production is constant with the season, studies have to find a way to predict for different pathways such as ebullition from emission from leaves, sediments, and import and export by the tidal water. During the study period, between July and August, the mangrove area was swamped with freshwater from the Coleroon River up to a depth of 90–120 cm. This suggests that when pneumatophores and soil are inundated, the gas transfer between the aerenchyma and the atmosphere is impeded and vice versa. The CH_4 efflux values ranged from 0.36 to 0.38 g CH_4 m^{-2} $month^{-1}$, which is lower than the June and September efflux estimates. Recently, a multiyear study of EC-based ecosystem CH_4 fluxes was examined for temporal variations and control of the biophysical drivers in estuarine mangroves of Hong Kong, China. The study found that the daily mangrove CH_4 flux peaked during the summer with the combination of higher temperature and lower salinity, whereas it was minor in the winter months (Liu et al. 2020).

Furthermore, the water level plays a significant role in determining soil temperature (Jha et al. 2014; Wang et al. 2016) and water salinity, and it was well correlated with the SEM (Fig. 8). Creek water parameters, particularly the increase in TOC concentration and sudden drop in water salinity from 40.5 in June to 11.5 in July, were also visualised and correlated in the present study (Figs. 7–8). Several studies revealed that the CH_4 fluxes were influenced by salinity (Purvaja and Ramesh 2001; Krithika et al. 2008; Dutta et al. 2013; Chauhan et al. 2015).

Salinity is one of the unique factors regulating the CH_4 flux in the mangroves wetlands; moreover, under hypersaline conditions, leaves have an adaptation strategy to reduce the transpiration process (Wu et al. 2012). Therefore, the mangrove plants can reduce transpiration, which significantly inhibits the CH_4 fluxes in the mangrove ecosystem. A good relationship was observed between creek water salinity and CH_4 flux in the present study. The hypersalinity reduces the CH_4 flux during the dry period. However, physiological controls and transport mechanisms are quite unclear for CH_4 fluxes in mangrove trees (Purvaja et al. 2004; He et al. 2019). The impact of tidal inundation on CH_4 efflux has a strong seasonal variation that can largely be attributed to the dry and wet seasons. The results of Jha et al. (2014) clarified that the emitted CH_4 flux during high tides was about 80% more than that during low tides. In contrast, the present study showed diurnal variability (Fig. 5).

Conclusions

This study reports CH_4 fluxes estimated using an EC technique in a South Indian tropical mangrove ecosystem. We have characterised the diurnal and seasonal patterns. Ecosystem-scale observations of the Pichavaram mangroves showed them to be a minor source for CH_4 during the wet season when compared with the dry season. The Pichavaram mangroves are also characterised by a lower emission rate than that seen in the tropical mangroves of Sundarbans, India, as well as in a subtropical forest near Hong Kong, China. Furthermore, statistical results indicate that air temperature, tidal inundation patterns, and water salinity were important for describing the variability of CH_4 flux in the site. Overall, the results suggest that the Pichavaram mangrove wetland acts as a minor source for CH_4. However, it may become a larger source as anthropogenic inputs of organic matter are increased and sea levels rise in the future. The study also has significance in quantifying the carbon sequestration rate of the wetland by eliminating the carbon lost through CH_4 emission. Hence, it is very important to have continuous, long-term data to understand the variations in CH_4 emission mechanisms under different environmental conditions.

Supplementary Information The online version contains supplementary material available at https://doi.org/10.1007/s12237-021-00988-1.

Acknowledgements This work is part of the MetFlux India Project initiated by the Indian Institute of Tropical Meteorology, Pune. The Ministry of Earth Sciences, Government of India, is acknowledged for financial support. We also thank the Tamil Nadu Forest Department for providing the necessary permission. We are grateful to the founder chairman and chairperson of the M. S. Swaminathan Research Foundation (MSSRF) for providing the facilities necessary for this work.

Funding We also appreciate the support from the National Natural Science Foundation of China (Grant No. U1602234); the CAS Key Laboratory of Tropical Forest Ecology, Xishuangbanna Tropical Botanical Garden, Chinese Academy of Sciences, China; the China Postdoctoral Science Foundation (Grant No. 2019M653512); and the Yunnan Postdoctoral Orientation Training Programme.

Declarations

Conflict of Interest The authors declare no competing interests.

References

Acosta, M., J. Dušek, S. Chamizo, et al. 2019. Autumnal fluxes of CH_4 and CO_2 from Mediterranean reed wetland based on eddy covariance and chamber methods. *Catena* 183:104191.

Alberto, M.C.R., R. Wassmann, R.J. Buresh, et al. 2014. Measuring methane flux from irrigated rice fields by eddy covariance method using open-path gas analyzer. *Field Crops Research* 160: 12–21.

Allen, D.E., R.C. Dalal, H. Rennenberg, et al. 2007. Spatial and temporal variation of nitrous oxide and methane flux between subtropical mangrove soils and the atmosphere. *Soil Biology and Biochemistry* 39: 622–631.

Allen, M.R., K.P. Shine, J.S. Fuglestvedt, et al. 2018. A solution to the misrepresentations of CO_2-equivalent emissions of short-lived climate pollutants under ambitious mitigation. *NPJ Climate and Atmospheric Science* 1: 16.

Atwood, T.B., R.M. Connolly, H. Almahasheer, et al. 2017. Global patterns in mangrove soil carbon stocks and losses. *Nature Climate Change* 7: 523–528.

Aubinet, M., T. Vesala, and D. Papale. 2012. *Eddy covariance: A practical guide to measurement and data analysis*. Dordrecht: Springer Science and Business Media.

Bai, Z., G. Yang, H. Chen, et al. 2014. Nitrous oxide fluxes from three forest types of the tropical mountain rainforests on Hainan Island China. *Atmospheric Environment* 92: 469–477.

Baldocchi, D.D. 1997. Measuring and modelling carbon dioxide and water vapour exchange over a temperate broad-leaved forest during the 1995 summer drought. *Plant Cell & Environment* 20: 1108–1122.

Baldocchi, D.D. 2003. Assessing the eddy covariance technique for evaluating carbon dioxide exchange rates of ecosystems: Past present and future. *Global Change Biology* 9: 479–492.

Baldocchi, D.D. 2014. Measuring fluxes of trace gases and energy between ecosystems and the atmosphere the state and future of the eddy covariance method. *Global Change Biology* 20: 3600–3609.

Baldocchi, D.D., E. Falge, L. Gu, et al. 2001. FLUXNET: A new tool to study the temporal and spatial variability of ecosystem–scale carbon dioxide water vapor and energy flux densities. *Bulletin of the American Meteorological Society* 82 (11): 2415–2434.

Baldocchi, D.D., J. Finnigan, K. Wilson, et al. 2000. On measuring net ecosystem carbon exchange over tall vegetation on complex terrain. *Boundary-Layer Meteorology* 96: 257–291.

Barnes J., R. Ramesh, R. Purvaja, et al. 2006. Tidal dynamics and rainfall control N_2O and CH_4 emissions from a pristine mangrove creek. *Geophysical Research Letters* 33.

Barr, J.G., V. Engel, J.D. Fuentes, et al. 2010. Controls on mangrove forest-atmosphere carbon dioxide exchanges in western Everglades National Park. *Journal of Geophysical Research: Biogeosciences* 115: G02020.

Biswas, H., S.K. Mukhopadhyay, S. Sen, et al. 2007. Spatial and temporal patterns of methane dynamics in the tropical mangrove dominated estuary NE coast of Bay of Bengal India. *Journal of Marine Systems* 68: 55–64.

Borges A.V., S. Djenidi, G. Lacroix, et al. 2003. Atmospheric CO_2 flux from mangrove surrounding waters. *Geophysical Research Letters* 30.

Bouillon, S., R.M. Connolly, and S.Y. Lee. 2008. Organic matter exchange and cycling in man- grove ecosystems: Recent insights from stable isotope studies. *Journal of Sea Research* 59: 44–58.

Cai, W., and Y. Wang. 1998. The chemistry fluxes and sources of carbon dioxide in the estuarine waters of the Satilla and Altamaha Rivers Georgia. *Limnology and Oceanography* 43 (4): 657–668.

Chakraborty, S., Y.K. Tiwari, P.K. Deb Burman, et al. 2020. Observations and modeling of GHG concentrations and fluxes over India. In: Krishnan R., Sanjay J., Gnanaseelan C., Mujumdar M., Kulkarni A., Chakraborty S. (eds) *Assessment of Climate Change over the Indian Region*. Singapore: Springer. https://doi.org/10.1007/978-981-15-4327-2.

Chang, T.C., and S.S. Yang. 2003. Methane emission from wetland in Taiwan. *Atmospheric Environment* 37: 4551–4558.

Chauhan, R., A. Datta, A.L. Ramanathan, et al. 2015. Factors influencing spatio- temporal variation of methane and nitrous oxide emission from a tropical mangrove of eastern coast of India. *Atmospheric Environment* 107: 95–106.

Chen, G.C., Y.I. Ulumuddin, S. Pramudji, et al. 2014. Rich soil carbon and nitrogen but low atmospheric greenhouse gas fluxes from North Sulawesi mangrove swamps in Indonesia. *Science of the Total Environment* 487: 91–96.

Deb Burman, P.K., D. Sarma, S. Chakraborty, et al. 2020. The effect of Indian summer monsoon on the seasonal variation of carbon sequestration by a forest ecosystem over North-East India. *SN Applied Sciences* 2 (2): 154.

Deb Burman, P. K., S. Launiainen, S. Mukherjee, et al. 2021. Ecosystem-atmosphere carbon and water exchanges of subtropical evergreen and deciduous forests in India. *Forest Ecology and Management* 495: 119371.

Donato, D.C., J.B. Kauffman, D. Murdiyarso, et al. 2011. Mangroves among the most carbon-rich forests in the tropics. *Nature Geoscience* 4 (5): 293.

Dutta, M.K., C. Chowdhury, T.K. Jana, et al. 2013. Dynamics and exchange fluxes of methane in the estuarine mangrove environment of the Sundarbans NE coast of India. *Atmospheric Environment* 77: 631–639.

Etheridge, D.M., L. Steele, R.J. Francey, et al. 1998. Atmospheric methane between 1000 AD and present: Evidence of anthropogenic emissions and climatic variability. *Journal of Geophysical Research: Atmospheres* 103: 15979–15993.

Etminan, M., G. Myhre, E.J. Highwood, et al. 2016. Radiative forcing of carbon dioxide, methane and nitrous oxide: A significant revision of the methane radiative forcing. *Geophysical Research Letters* 43: 12–614.

Fang, K., X. Yi, W. Dai, et al. 2019. Effects of integrated rice-frog farming on paddy field greenhouse gas emissions. *International Journal of Environmental Research and Public Health* 16 (11): 1930.

Foken, T., M. Göckede, M. Mauder, et al. 2004. Post field data quality control. In Handbook of Micrometeorology: A Guide for Surface Flux Measurement and Analysis, eds. X Lee, W Massman, and B Law (Eds.). 81–108. Dordrecht: Kluwer.

Fortuniak, K., W. Pawlak, L. Bednorz, et al. 2017. Methane and carbon dioxide fluxes of a temperate mire in Central Europe. *Agricultural and Forest Meteorology* 232: 306–318.

Ganesan, A.L., M. Rigby, M.F. Lunt, et al. 2017. Atmospheric observations show accurate reporting and little growth in India's methane emissions. *Nature Communications* 8: 836.

Ge, H.X., H.S. Zhang, H. Zhang, et al. 2018. The characteristics of methane flux from an irrigated rice farm in East China measured using the eddy covariance method. *Agricultural and Forest Meteorology* 249: 228–238.

Gedney, N., P.M. Cox, and C. Huntingford. 2004. Climate feedback from wetland methane emissions. *Geophysical Research Letters* 31: L20503.

Gnanamoorthy, P., V. Selvam, P., Deb Burman, et al. 2020. Seasonal variations of net ecosystem (CO_2) exchange in the Indian tropical mangrove forest of Pichavaram. *Estuarine Coastal and Shelf Science* 243: 106828.

Gnanamoorthy, P., V. Selvam, R. Ramasubramanian, et al. 2019. Diurnal and seasonal patterns of soil CO_2 efflux from the Pichavaram mangroves India. *Environmental Monitoring and Assessment* 191: 258.

Göckede, M., T. Foken, M. Aubinet, et al. 2008. Quality control of CarboEurope flux data - Part 1: Coupling footprint analyses with flux data quality assessment to evaluate sites in forest ecosystems. *Biogeosciences* 5 (2): 433–450.

Gran, G. 1952. Determination of the equivalence point in potentiometric titrations Part II. *The Analyst* 77 (920): 661–671.

Großkopf, R., P.H. Janssen, and W. Liesack. 1998. Diversity and structure of themethanogenic community in anoxic rice paddy soil microcosms as examined by cultivation and direct 16S rRNA gene sequence retrieval. *Applied and Environmental Microbiology* 64: 960–969.

Guha, T., Y.K. Tiwari, and V. Valsala. 2018. What controls the atmospheric methane seasonal variability over India? *Atmospheric Environment* 175: 83–91.

Hatala, J.A., M. Detto, and D.D. Baldocchi. 2012a. Gross ecosystem photosynthesis causes a diurnal pattern in methane emission from rice. *Geophysical Research Letters* 39.

Hatala, J.A., M. Detto, O. Sonnentag, et al. 2012b. Greenhouse gas (CO_2 CH_4 H_2O) fluxes from drained and flooded agricultural peatlands in the Sacramento-San Joaquin Delta. *Agriculture Ecosystems & Environment* 150: 1–18.

He, Y., W. Guan, D. Xue, et al. 2019. Comparison of methane emissions among invasive and native mangrove species in Dongzhaigang Hainan Island. *Science of the Total Environment* 697: 133945.

Hou, J.T., Z.L. Wen, and Z.J. Cheng. 2004. Structural equation model and its application. Beijing: Beijing Educational Science Publishing House.

IMD (India Meteorological Department). 1973. Northeast monsoon. *Forecasting manual report* IV 18: 4.

IPCC (Intergovernmental Panel on Climate Change). 2013. Climate change 2013: the physical science basis. In: Contribution of Working Group I to the Fifth Assessment Report of the Intergovernmental Panel on Climate Change, eds. TF Stocker, D Qin, GK Plattner, M Tignor, SK Allen, J Boschung, A Nauels, Y Xia, V Bex, PM Midgley. New York: Cambridge University Press.

Jacotot, A., C. Marchand, and M. Allenbach. 2018. Tidal variability of CO_2 and CH_4 emissions from the water column within a Rhizophora mangrove forest (New Caledonia). *Science of the Total Environment* 631: 334–340.

Jha, C.S., S.R. Rodda, K.C. Thumaty, et al. 2014. Eddy covariance based methane flux in Sundarbans mangroves India. *Journal of Earth System Science* 123 (5): 1089–1096.

Jiang, L.Q., W.J. Cai, and Y. Wang. 2008. A comparative study of carbon dioxide degassing in river- and marine-dominated estuaries. *Limnology and Oceanography* 53: 2603–2615.

Kathiresan, K. 2000. A review of studies on Pichavaram mangrove Southeast India. *Hydrobiologia* 430: 185–205.

Kljun, N., P. Calanca, M.W. Rotach, et al. 2004. A simple parameterisation for flux footprint predictions. *Boundary-Layer Meteorology* 112: 503–523.

Knox, S.H., R.B. Jackson, B. Poulter, et al. 2019. FluXNET-CH_4 synthesis activity objectives, observations, and future directions. *Bulletin of the American Meteorological Society* 100 (12): 2607–2632.

Konnerup, D., J.M. Betancourt-Portela, C. Villamil, et al. 2014. Nitrous oxide and methane emissions from the restored mangrove ecosystem of the Cienaga Grande de Santa Marta Colombia. *Estuarine Coastal and Shelf Science* 140: 43–51.

Kormann, R., and F.X. Meixner. 2001. An analytical footprint model for non-neutral stratification. *Boundary-Layer Meteorology* 99: 207–224.

Kristensen, E., S. Bouillon, T. Dittmar, et al. 2008a. Organic carbon dynamics in mangrove ecosystems: A review. *Aquatic Botany* 89: 201–219.

Kristensen, E., M.R. Flindt, S. Ulomi, et al. 2008b. Emission of CO_2 and CH_4 to the atmosphere by sediments and open waters in two Tanzanian mangrove forests. *Marine Ecology Progress Series* 370: 53–67.

Krithika, K., R. Purvaja, and R. Ramesh. 2008. Fluxes of methane and nitrous oxide from an Indian mangrove. *Current Science* 94: 218–224.

Krupadam, R.J., R. Ahuja, S.R. Wate, et al. 2007. Forest bound estuaries are higher methane emitters than paddy fields: A case of Godavari estuary East Coast of India. *Atmospheric Environment* 41: 4819–4827.

Lekphet, S., S. Nitisoravut, and S. Adsavakulchai. 2005. Estimating methane emission from mangrove area in Ranong Province Thailand. *Songklanakarin Journal of Science and Technology* 27: 153–163.

Liu, J., Y. Zhou, A. Valach, et al. 2020. Methane emissions reduce the radiative cooling effect of a subtropical estuarine mangrove wetland by half. *Global Change Biology* 26 (9): 4998–5016.

Livesley, S.J., and S.M. Andrusiak. 2012. Temperate mangrove and salt marsh sediments are a small methane and nitrous oxide source but important carbon store. *Estuarine Coastal and Shelf Science* 97: 19–27.

Livingston, G.P., and G.L. Hutchinson. 1995. Enclosure-based measurement of trace gas exchange: Applications and sources of error. In *Biogenic trace gases: Measuring emissions from soil and water*, ed. P.A. Matson and R.C. Harris, 14–51. Oxford: Blackwell Science Ltd.

Lyimo, T.J., A. Pol, and H.J.M. Op den Camp. 2002. Methane emission sulphide concentration and redox potential profiles in Mtoni mangrove soil Tanzania. *Western Indian Ocean Journal of Marine Science* 1: 71–80.

Ma, S., J. Jiang, Y. Huang, et al. 2017. Data-constrained projections of methane fluxes in a northern minnesota peatland in response to elevated CO_2 and warming. *Journal of Geophysical Research: Biogeosciences* 122: 2841–2861.

McNicol, G., C.S. Sturtevant, S.H. Knox, et al. 2017. Effects of seasonality transport pathway and spatial structure on greenhouse gas fluxes in a restored wetland. *Global Change Biology* 23: 2768–2782.

Meijide, A., G. Manca, I. Goded, et al. 2011. Seasonal trends and environmental controls of methane emissions in a rice paddy field in Northern Italy. *Biogeosciences* 8: 3809–3821.

Metya, A., A. Datye, S. Chakraborty, et al. 2021a. Diurnal and seasonal variability of CO_2 and CH_4 concentrations in a semi-urban environment of western India. *Scientific Reports* 11: 2931.

Metya, A., S. Chakraborty, S.K. Bhattacharya, et al. 2021b. Isotopic and concentration analyses of CO_2 and CH_4 in association with the eddy-covariance based measurements in a tropical forest of northeast India. *Earth and Space Science* 8(6): e2020EA001504.

Morin, T.H. 2018. Advances in the eddy covariance approach to CH_4 monitoring over two and a half decades. *Journal of Geophysical Research: Biogeosciences* 124: 453–460.

Mukhopadhyay, S.K., H. Biswas, T.K. De, et al. 2002. Impact of Sundarban mangrove biosphere on the carbon dioxide and methane mixing ratios at the NE Coast of Bay of Bengal India. *Atmospheric Environment* 36: 629–638.

Myhre, G., D. Shindell, F.M. Bréon, et al. 2013. Anthropogenic and natural radiative forcing. In *Climate change 2013: The physical science basis: Contribution of working group I to the Fifth Assessment Report of the Intergovernmental Panel on Climate Change*, ed. T.F. Stocker, D. Qin, G.K. Plattner, M. Tignor, S.K. Allen, J. Boschung, A. Nauels, Y. Xia, V. Bex, and P.M. Midgley, 659–740. Cambridge: Cambridge University Press.

Nemitz, E., I. Mammarella, A. Ibrom, et al. 2018. Standardisation of eddy-covariance flux measurements of methane and nitrous oxide. *International Agrophysics* 32 (4): 517–549.

Nisbet, E.G., E.J. Dlugokencky, M.R. Manning, et al. 2016. Rising atmospheric methane: 2007–2014 growth and isotopic shift. *Global Biogeochemical Cycles* 30 (9): 1356–1370.

Nisbet, E.G., M.R. Manning, E.J. Dlugokencky, et al. 2019. Very strong atmospheric methane growth in the 4 years 2014–2017: Implications for the Paris agreement. *Global Biogeochemical Cycles* 33 (3): 318–342.

Nobrega, G.N., T.O. Ferreira, M.S. Neto, et al. 2016. Edaphic factors controlling summer (rainy season) greenhouse gas emissions (CO_2 and CH_4) from semiarid mangrove soils (NE-Brazil). *Science of the Total Environment* 542: 685–693.

Papale, D., M. Reichstein, M. Aubinet, et al. 2006. Towards a standardized processing of net ecosystem exchange measured with eddy covariance technique: Algorithms and uncertainty estimation. *Biogeosciences* 3 (4): 571–583.

Pavelka, M., P. Sedľak, M. Acosta, et al. 2007. Chamber techniques versus eddy covariance method during nighttime measurements. In *International Scientific Conference, Slovakia*.

Peterson, B.G., P. Carl, K. Boudt, et al. 2018. Package 'performance analytics'. R Team Cooperation.

Petrescu, A.M.R., A. Lohila, J.P. Tuovinen, et al. 2015. The uncertain climate footprint of wetlands under human pressure. *Proceedings of the National Academy of Sciences* 112: 4594–4599.

Purvaja, R., and R. Ramesh. 2001. Natural and anthropogenic methane emission from coastal wetlands of South India. *Environmental Management* 27: 547–557.

Purvaja, R., R. Ramesh, and P. Frenzel. 2004. Plant-mediated methane emission from Indian mangroves. *Global Change Biology* 10: 1825–1834.

Rajeevan, M., C.K. Unnikrishnan, K. JyotiBhate, et al. 2012. Northeast monsoon over India: Variability and prediction. *Meteorological Applications* 19: 226–236.

Reichstein, M., E. Falge, D.D. Baldocchi, et al. 2005. On the separation of net ecosystem exchange into assimilation and ecosystem respiration: Review and improved algorithm. *Global Change Biology* 11 (9): 1424–1439.

Rinne, J., T. Riutta, M. Pihlatie, et al. 2007. Annual cycle of methane emission from a boreal fen measured by the eddy covariance technique. *Tellus B: Chemical and Physical Meteorology* 59: 449–457.

Rosentreter, J.A., D.T. Maher, D.V. Erler, et al. 2018. Methane emissions partially offset "blue carbon" burial in mangroves. *Science Advances* 4: eaao498.

Rosentreter, J.A., A.V. Borges, B.R. Deemer, et al. 2021. Half of global methane emissions come from highly variable aquatic ecosystem sources. *Nature Geoscience* 14 (4): 225–230.

Sabbatini, S., I. Mammarella, N. Arriga, et al. 2018. Eddy covariance raw data processing for CO_2 and energy fluxes calculation at ICOS ecosystem stations. *International Agrophysics* 32: 495–515.

Saunois, M., P. Bousquet, B. Poulter, et al. 2017. Variability and quasi-decadal changes in the methane budget over the period 2000–2012. *Atmospheric Chemistry and Physics* 17: 11135–11161.

Saunois, M., A.R. Stavert, and B. Poulter. 2020. The global methane budget 2000–2017. *Earth System Science Data* 12: 1561–1623.

Schwarz, J.I., W. Eckert, and R. Conrad. 2007. Community structure of archaea and bacteria in a profundal lake sediment Lake Kinneret (Israel). *Systematic and Applied Microbiology* 30: 239–254.

Senthilkumar, B. 2008. *Biogeochemical and biophysical aspects of Pichavaram mangrove ecosystem South India*. Chennai: Anna University PhD thesis (Unpublished).

Selvam, V. 2003. Environmental classification of mangrove wetlands of India. *Current Science* 84: 759–765.

Selvam, V., L. Gnanappazham, M. Navamuniyammal, et al. 2002. Atlas of mangrove wetlands of India. Chennai: *M.S. Swaminathan Research Foundation* 12–58.

Siikamäki, J., J.N. Sanchirico, and S.L. Jardine. 2012. Global economic potential for reducing carbon dioxide emissions from mangrove loss. *Proceedings of the National Academy of Sciences* 109 (36): 14369–14374.

Sotomayor, D., J.E. Corredor, and J.M. Morell. 1994. Methane flux from mangrove sediments along the Southwestern Coast of Puerto Rico. *Estuaries* 17: 140–147.

Sreenivas, G., P. Mahesh, J. Subin, et al. 2016. Influence of meteorology and interrelationship with greenhouse gases (CO_2 and CH_4) at a suburban site of India. *Atmospheric Chemistry and Physics* 16: 3953–3967.

Strickland, J.D.H., and T.R. Parsons, 1972. A practical handbook of seawater analysis. *Fisheries Research Board of Canada Bulletin* 157 (2): 310.

Tang, A.C.I., P.C. Stoy, R. Hirata, et al. 2018. Eddy covariance measurements of methane flux at a tropical peat forest in Sarawak Malaysian Borneo. *Geophysical Research Letters* 45: 4390–4399.

Tiwari, Y.K., T. Guha, V. Valsala, et al. 2020. Understanding atmospheric methane sub-seasonal variability over India. *Atmospheric Environment* 223: 117206.

Turner, A.J., C. Frankenberg, and E.A. Kort. 2019. Interpreting contemporary trends in atmospheric methane. *Proceedings of the National Academy of Sciences* 116: 2805–2813.

Walkley, A., and I.A. Black. 1934. An examination of the Degtjareff method for determining soil organic matter and a proposed modification of the chromic acid titration method. *Soil Science* 37: 29–38.

Wang, H.T., G.S. Liao, M. D'Souza, et al. 2016. Temporal and spatial variations of greenhouse gas fluxes from a tidal mangrove wetland in Southeast China. *Environmental Science and Pollution Research* 23: 1873–1885.

Webb, E.K., G.I. Pearman, and R. Leuning. 1980. Correction of flux measurements for density effects due to heat and water vapour transfer. *Quarterly Journal of the Royal Meteorological Society* 106: 85–100.

Wilczak, J.M., S.P. Oncley, and S.A. Stage. 2001. Sonic anemometer tilt correction algorithms. *Boundary-Layer Meteorology* 99: 127–150.

Wille, C., L. Kutzbach, T. Sachs, et al. 2008. Methane emission from Siberian arctic polygonal tundra: Eddy covariance measurements and modelling. *Global Change Biology* 14 (6): 1395–1408.

Wu, T., C. Ye, and W. Han. 2012. Leaf anatomical structure and its ecological adaptability of five species of Rhizophoraceae plants. *Bulletin of Botanical Research* 32: 143–146 (in Chinese with an English abstract).

Wutzler, T., A. Lucas-Moffat, M. Migliavacca, et al. 2018. Basic and extensible post-processing of eddy covariance flux data with REddyProc. *Biogeosciences* 15: 5015–5030.

Wylie, L., A.E. Sutton-Grier, and A. Moore. 2016. Keys to successful blue carbon projects: Lessons learned from global case studies. *Marine Policy* 65: 76–84.

Zhang, Z., N.E. Zimmermann, A. Stenke, et al. 2017. Emerging role of wetland methane emissions in driving 21st century climate change. *Proceedings of the National Academy of Sciences* 114: 9647–9652.

Zheng, X., J. Guo, W. Song, et al. 2018. Methane emission from mangrove wetland soils is marginal but can be stimulated significantly by anthropogenic activities. *Forests* 9 (12): 738.

Zhu, Z., X. Sun, X. Wen, et al. 2006. Study on the processing method of nighttime CO_2 eddy covariance flux data in China FLUX. *Science in China Series D: Earth Sciences* 49: 36–46.